

Supplemental Information

Inhibition of ATPIF1 ameliorates severe mitochondrial respiratory chain dysfunction in mammalian cells

Walter W Chen^{1-4,*}, Kivanc Birsoy^{1-4,*}, Maria M Mihaylova¹⁻⁴, Harriet Snitkin⁶, Iwona Stasinski⁶,
Burcu Yucel¹⁻⁴, Erol C Bayraktar¹⁻⁴, Jan E Carette⁷, Clary B Clish³, Thijn R Brummelkamp⁸, David
D Sabatini⁶ and David M Sabatini¹⁻⁵

¹Whitehead Institute for Biomedical Research, Nine Cambridge Center, Cambridge, MA 02142, USA.

²Department of Biology, Massachusetts Institute of Technology (MIT), Cambridge, MA 02139, USA.

³Broad Institute, Seven Cambridge Center, Cambridge, MA 02142, USA.

⁴David H. Koch Institute for Integrative Cancer Research at MIT, 77 Massachusetts Avenue, Cambridge, MA 02139, USA.

⁵Howard Hughes Medical Institute, MIT, Cambridge, MA 02139, USA.

⁶Department of Cell Biology, New York University School of Medicine, New York, New York, 10016, USA.

⁷Department of Microbiology and Immunology, Stanford University School of Medicine, Stanford, CA 94305, USA.

⁸Department of Biochemistry, Netherlands Cancer Institute, Plesmanlaan 121 1066 CX, Amsterdam, The Netherlands.

To whom correspondence should be addressed. Email: sabatini@wi.mit.edu

* These authors contributed equally to this work.

INVENTORY OF SUPPLEMENTAL INFORMATION

Figure S1: Knockdown of ATPIF1 protects KBM7 cells against antimycin. Relates to Figure 1.

Figure S2: Loss of ATPIF1 leads to increased depletion of glycolytic intermediates during antimycin treatment. Relates to Figure 1.

Figure S3: Loss of ATPIF1 does not alter general aspects of cellular and mitochondrial physiology. Relates to Figure 1.

Figure S4: Generation of *ATPIF1*^{-/-} mice and characterization of derived primary hepatocytes. Relates to Figure 4.

Table S1: Raw metabolite profiling data from experiments comparing WT and ATPIF1_KO KBM7 cells under antimycin treatment. Relates to Figure 1.

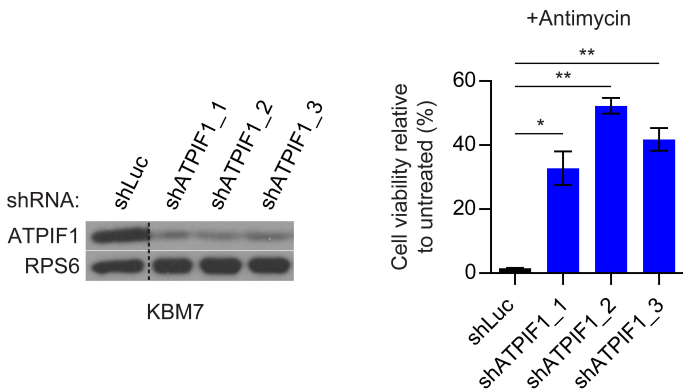


Figure S1, related to Figure 1: Knockdown of ATPIF1 protects KBM7 cells against antimycin

Shown on the left are the immunoblots for indicated proteins of WT KBM7 cells expressing control shLuc or shRNAs targeting ATPIF1 (shATPIF1_1, shATPIF1_2, shATPIF1_3). Dotted vertical line indicates that the first lane and the other three lanes were from the same immunoblot but were not adjacent. Shown on the right is the viability of WT KBM7 cells expressing shLuc, shATPIF1_1, shATPIF1_2, or shATPIF1_3 when treated with antimycin (100 μ M) for 3 days, as determined by CellTiter-Glo. Error bars are \pm s.e.m. (n = 2). * P < 0.05, ** P < 0.01.

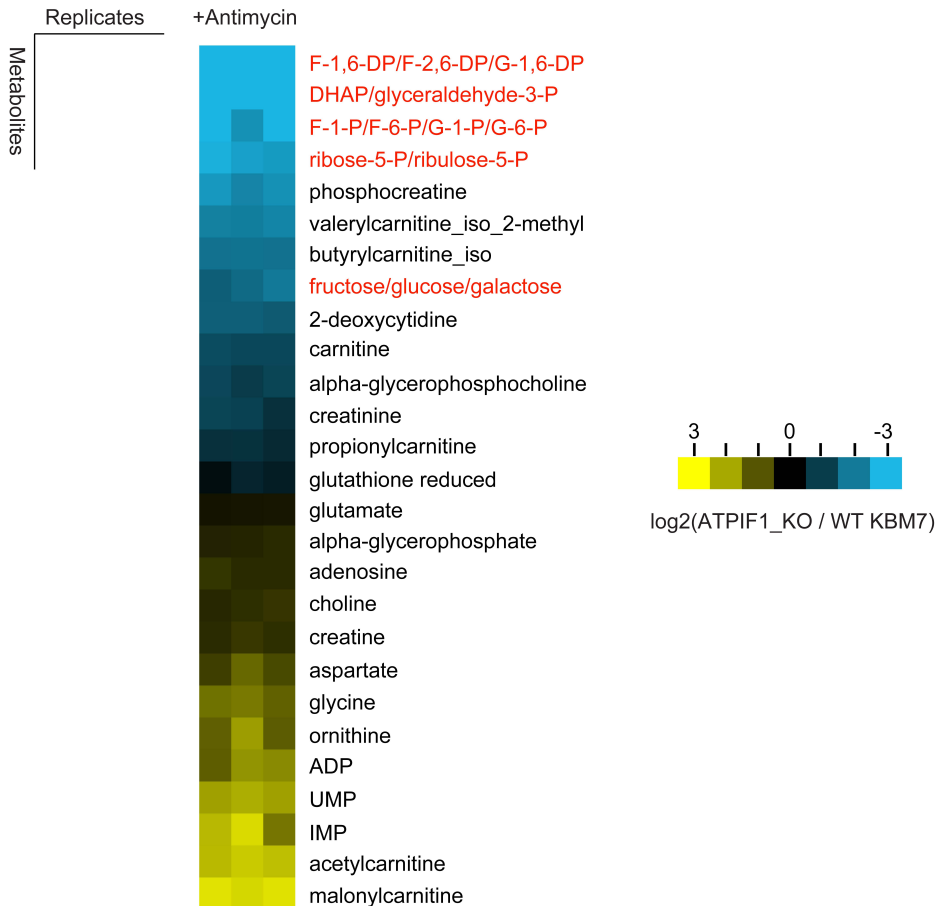


Figure S2, related to Figure 1: Loss of ATPIF1 leads to increased depletion of glycolytic intermediates during antimycin treatment

Shown is a heatmap of all metabolites with significant differences ($P < 0.01$) in the amounts found in ATPIF1_KO and WT KBM7 cells after 1 hour of treatment with antimycin ($120 \mu\text{M}$). Each row represents a metabolite and each column represents a biological replicate. Glycolytic intermediates are highlighted in red.

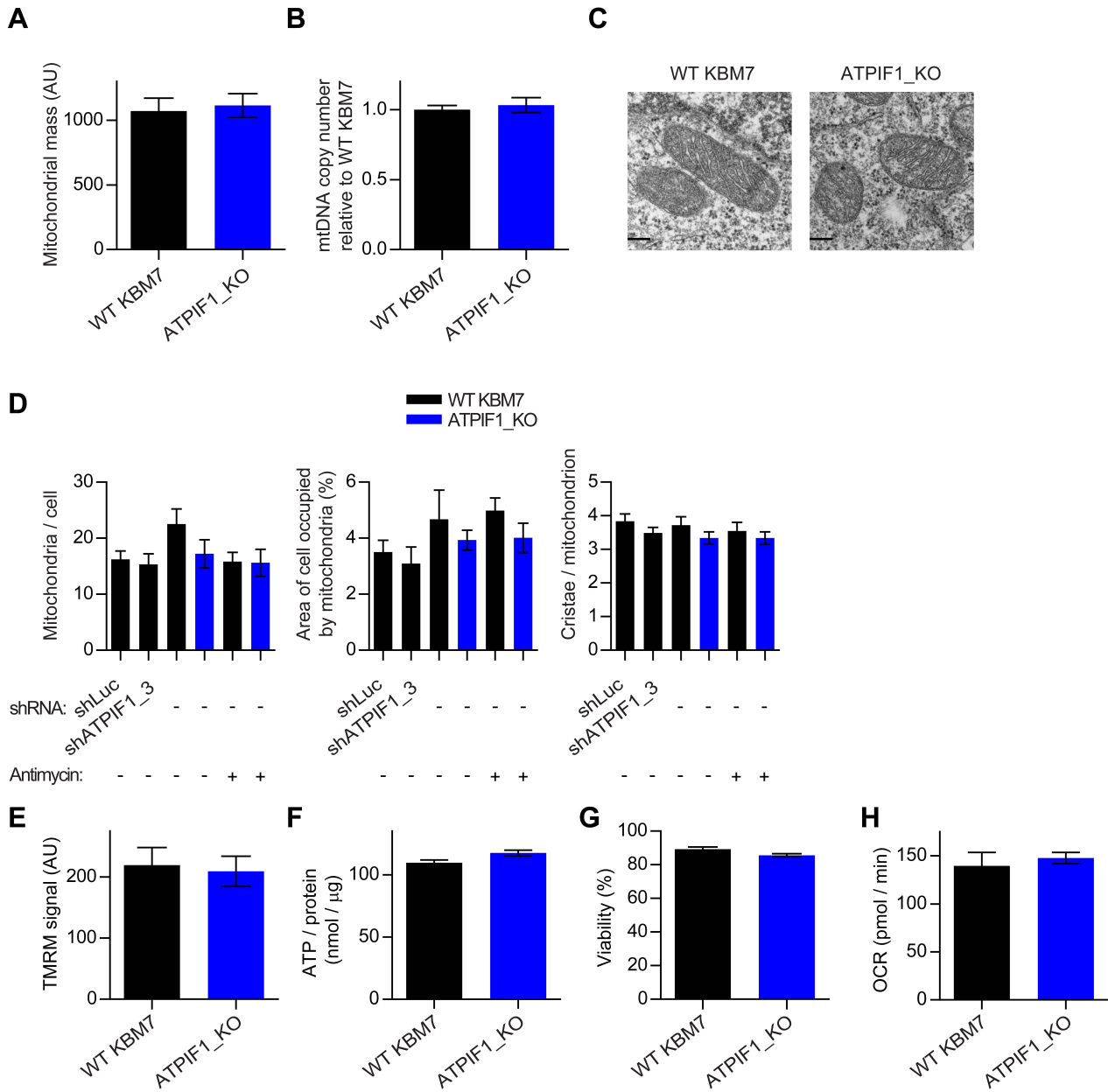


Figure S3, related to Figure 1: Loss of ATPIF1 does not alter general aspects of cellular and mitochondrial physiology

(A) Mitochondrial mass of WT and ATPIF1_KO KBM7 cells as determined by MitoTracker Green FM staining. (B) mtDNA copy number of WT and ATPIF1_KO KBM7 cells. (C) Representative EM micrographs of WT and ATPIF1_KO KBM7 cells. Scale bars, 200 nm. (D) Quantitative EM analysis of mitochondria in WT and ATPIF1_KO KBM7 cells. Shown are data for WT KBM7 cells expressing control shLuc or shATPIF1_3, and uninfected WT and ATPIF1_KO KBM7 cells with and without treatment with 125 μ M antimycin for 3 hours. Error bars are \pm s.e.m. ($n = 10$). (E) TMRM staining of WT and ATPIF1_KO KBM7 cells as determined by FACS. (F) Cellular ATP of WT and ATPIF1_KO KBM7 cells. (G) Viability of untreated WT and ATPIF1_KO KBM7 cells as determined by 7-AAD staining. (H) Oxygen consumption rate (OCR) of WT and ATPIF1_KO KBM7 cells. Error bars are \pm s.e.m. ($n = 3$), unless otherwise indicated.

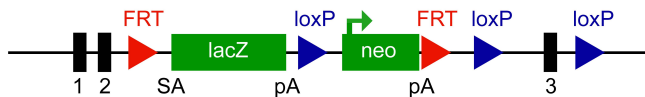
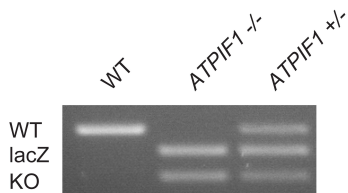
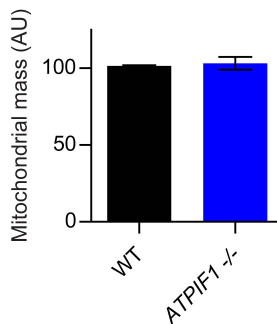
A**B****C**

Figure S4, related to Figure 4: Generation of *ATPIF1*^{-/-} mice and characterization of derived primary hepatocytes

(A) Schematic of gene-trap knockout design. The presence of a splice acceptor (SA) site downstream of exon 2 leads to the generation of transcripts lacking exon 3. Mice homozygous for the gene-trap allele are constitutive knockouts but can be converted to conditional knockouts through the activity of FLP recombinase. Conditional knockouts can then be manipulated with Cre recombinase. Black bars represent exons 1, 2, 3 of *ATPIF1*. FRT = FLP recombinase sites, loxP = Cre recombinase sites, lacZ = lacZ cassette, neo = neoR cassette, SA = splice acceptor site, pA = polyadenylation signal. (B) Genotyping PCR of WT, *ATPIF1*^{-/-}, and *ATPIF1*^{+/-} mice. WT = native *ATPIF1* allele, lacZ = lacZ cassette, KO = gene-trap *ATPIF1* allele. (C) Mitochondrial mass of WT and *ATPIF1*^{-/-} primary hepatocytes as determined by MitoTracker Green FM staining. Error bars are \pm s.e.m. (n = 3).

SUPPLEMENTAL EXPERIMENTAL PROCEDURES

Materials. Materials were obtained from the following sources: antibodies to ATPIF1 and ATP5B from Sigma-Aldrich; antibodies to RAPTOR, RPS6 from Cell Signaling Technologies; antibody to β -actin, and HRP-conjugated anti-mouse, anti-rabbit, and anti-goat secondary antibodies from Santa Cruz Biotechnology; antimycin, tigecycline, ddl, verapamil, polybrene, puromycin, ATP, and uracil from Sigma-Aldrich; piericidin from Enzo Life Sciences; blasticidin from Invivogen; MitoTracker Green FM, TMRM, and 7-AAD from Invitrogen; DMEM, RPMI-1640 media from Sigma; IMDM from US Biologicals; Medium 199 and GlutaMAX from Invitrogen. All cell lines were obtained from ATCC.

DNA constructs. The ORF of ATPIF1 isoform 1 was cloned into the lentiviral vector, PLJM1-puro, and the retroviral vector, pMXs-IRES-blasticidin, using the following primers: PLJM1_ATPIF1_F, ATT ACC GGT ATG GCA GTG ACG GCG TTG; PLJM1_ATPIF1_R, ATT GAA TTC TTA ATC ATC ATG TTT TAG CAT TTT GAT CTT CTG C; pMXs_ATPIF1_F, ATG GAT CCG CCA CCA TGG CAG TGA CGG CGT TG; pMXs_ATPIF1_R, ATG CGG CCG CTT AAT CAT CAT GTT TTA GCA TTT TGA TCT TCT GCT TAT GG. pljm1-Flag-RAP2A was obtained from Addgene. The E55A mutation was generated using site-directed mutagenesis with a QuikChange II XL kit (Stratagene) and the following primers: E55A_F, GAG AGA GCA GGC TGA AGC GGA ACG ATA TTT CCG AG; E55A_R, CTC GGA AAT ATC GTT CCG CTT CAG CCT GCT CTC TC. Lentiviral shRNAs were obtained from The RNAi Consortium (TRC) collection of the Broad Institute. The TRC numbers for the shRNAs used are as follows: shLuc (TRCN0000072249), shATPIF1_1 (TRCN0000146646), shATPIF1_2 (TRCN0000150110), shATPIF1_3 (TRCN0000149949).

Cell culture and virus transduction. KBM7 cells were cultured in IMDM supplemented with 10% IFS and penicillin/streptomycin, except for studies using tigecycline in which they were

cultured in RPMI-1640. SH-SY5Y, HeLa, Malme-3M cells were cultured in DMEM supplemented with 10% FBS and penicillin/streptomycin. HeLa WT, HeLa ρ^0 , and KBM7 cells used for *ddl* experiments were grown in DMEM supplemented with 10% FBS, penicillin/streptomycin, and 100 $\mu\text{g}/\text{mL}$ uridine. Primary hepatocytes were cultured in Medium 199 supplemented with 10% FBS, penicillin/streptomycin, and GlutaMAX. KBM7, HeLa WT, and HeLa ρ^0 cells stably overexpressing ATPIF1 (WT or E55A) were generated via infection with retroviruses and selected with blasticidin (10 $\mu\text{g}/\text{mL}$) for three days. Malme-3M cells stably overexpressing RAP2A or ATPIF1 were generated by infection with lentiviruses expressing the corresponding cDNAs, followed by selection with puromycin (2 $\mu\text{g}/\text{mL}$) for three days. KBM7, SH-SY5Y, and HeLa cells expressing shLuc or shATPIF1 were generated by infection with lentiviruses expressing the corresponding shRNAs. All cells were infected with spin-infection using a 30 minute spin at 2,250 rpm in media containing polybrene (4 $\mu\text{g}/\text{mL}$), followed by selection one day later.

Haploid cell screening. Haploid cell genetic screening with antimycin was performed using 100 million mutagenized KBM7 cells, as described previously (Birsoy et al., 2013, Carette et al., 2011). Briefly, mutagenized haploid KBM7 cells were treated with antimycin (135 μM) for 3 weeks. Genomic DNA was isolated from pooled surviving clones and insertions were amplified. The sequences flanking retroviral insertion sites were mapped to the human genome using inverse PCR followed by Illumina sequencing. The statistical enrichment of insertions at a given locus in the selected population was calculated by comparing the number of inactivating insertions to those in the untreated control data set via Fisher's exact test and plotted. Individual clones were simultaneously isolated and tested by immunoblotting after the screen was finished.

Metabolic assays. For ATP assays, 100,000 cells were seeded, treated with the indicated amounts of drugs for the indicated amounts of time, and relative ATP levels compared to

untreated cells were determined using a luciferase-based assay (Promega). When measuring absolute cellular ATP levels, ATP standards were run and cellular ATP levels were ultimately normalized to cellular protein levels, which were determined by Bradford assay. For measurements of metabolites, 10 million WT and ATP1F1_KO KBM7 cells were cultured in the presence of DMSO or antimycin (120 μ M) for 1 hour or 8 hours. Afterwards, cells were quickly washed three times with cold PBS and the metabolites extracted by addition of 80% ice-cold methanol followed by incubation on dry ice for 15 minutes. Intracellular metabolite profiles were obtained using LC-MS as described previously (Finley et al., 2012).

Electron microscopy. KBM7 cells were fixed in 2% glutaraldehyde in 0.1 M sodium cacodylate buffer pH 7.4 at room temperature. After post-fixation in 2% OsO₄, blocks were processed for embedding in Epon 812. Thin sections were obtained, stained with uranyl acetate and lead citrate, and examined by transmission electron microscopy in a JEOL EX 1200 electron microscope. For each cell type, we analyzed 10 representative electron micrographs corresponding to sections (whole cell profiles) that went through the nucleus. For each of the 10 cells, we took a low magnification (5000X) electron micrograph from which we counted the number of mitochondria and measured the area of the cell using Image J from the NIH. We then marked each mitochondrion and took individual high magnification (40,000X) electron micrographs of all the mitochondria in the cell profile. In these 40,000X micrographs, we measured the area and cristae number of each mitochondrion.

Seahorse analysis. Oxygen consumption of intact cells was measured using an XF24 Extracellular Flux Analyzer (Seahorse Bioscience). For suspension cells, Seahorse plates were coated with Cell TAK (BD, 0.02mg/ml in 0.1 μ M NaHO₃) for 20 minutes to increase adherence of suspension cells. 300,000 cells were then attached to the plate by centrifugation at 2200 rpm without brakes for 5 min. IMDM was used as the assay media for all experiments.

Immunoblots. Cells were washed twice with ice-cold PBS and harvested in standard RIPA buffer containing Complete EDTA-free protease inhibitor (Roche). Proteins from total lysates were resolved by 12-16% SDS-PAGE and analyzed by immunoblotting using the indicated antibodies (1:1000).

Q-PCR and Q-RT-PCR assays. For analysis of mtDNA copy number, genomic and mitochondrial DNA were extracted from cells using the QIAamp DNA mini kit according to the manufacturer's instructions (Qiagen). For analysis of mRNA levels, RNA was extracted from cells using the RNeasy Plus Mini Kit according to the manufacturer's instructions (Qiagen) and reverse-transcribed to cDNA. Q-PCR was performed using the SYBR Green PCR Master Mix according to the manufacturer's instructions (Invitrogen). Primers targeting the mitochondrial gene *ND1* and the nuclear gene *RUNX2* were used to assess mtDNA copy number by normalizing ct values of *ND1* to those of *RUNX2*: *ND1_F*, CCC TAA AAC CCG CCA CAT CT; *ND1_R*, GAG CGA TGG TGA GAG CTA AGG T; *RUNX2_F*, CGC ATT CCT CAT CCC AGT ATG; *RUNX2_R*, AAA GGA CTT GGT GCA GAG TTC AG. Primers targeting *ATPIF1* and *ACTB* mRNA were used to assess *ATPIF1* mRNA levels by normalizing ct values of *ATPIF1* to those of *ACTB*: *ATPIF1_mRNA_F*, CTT CGG CTC GGA TCA GTC; *ATPIF1_mRNA_R*, CTG CCA GTT GTT CTC TAC TCT G; *ACTB_mRNA_F*, CCC TGG CAC CCA GCA C; *ACTB_mRNA_R*, GCC GAT CCA CAC GGA GTA C. Relative differences between samples were determined using the comparative Ct method.

***ATPIF1* ^{-/-} mice.** All animal studies and procedures were approved by the MIT Institutional Animal Care and Use Committee. *ATPIF1* ^{-/-} C57BL/6N mice were obtained from the International Knockout Mouse Consortium (Brown and Moore, 2012) and maintained on a standard light-dark cycle with food and water *ad libitum*. Genotyping primers were designed to distinguish between the native WT allele, the gene-trap allele, and the *lacZ* cassette:
ATPIF1_geno_F, CGG AAA AAC AGC AGG GAA AT; *ATPIF1_geno_R*, GGC ATT GGA CTG

GGG TTT AC; lacZ_genotype_F, ATT AGG GCC GCA AGA AAA CT; lacZ_genotype_R, CTG TAG CGG CTG ATG TTG AA. PCR with ATP1F1_genotype_F, ATP1F1_genotype_R gives a 221 bp product for the WT allele and a 163 bp product for the gene-trap allele. PCR with lacZ_genotype_F and lacZ_genotype_R gives a 192 bp product for the lacZ cassette.

Primary hepatocyte cultures. Primary hepatocytes were isolated from 8 – 18 week old mice with the indicated genotypes by collagenase perfusion. Prior to plating, cells were incubated with ACK (Ammonium-Chloride-Potassium) lysing buffer for two minutes to eliminate red blood cells. Cells were maintained in Medium 199 supplemented with 10% FBS, penicillin/streptomycin, and GlutaMAX. Media was changed daily and cells were treated as indicated.

SUPPLEMENTAL REFERENCES

- Birsoy, K., Wang, T., Possemato, R., Yilmaz, O. H., Koch, C. E., Chen, W. W., Hutchins, A. W., Gultekin, Y., Peterson, T. R., Carette, J. E., Brummelkamp, T. R., Clish, C. B. & Sabatini, D. M. 2013. MCT1-mediated transport of a toxic molecule is an effective strategy for targeting glycolytic tumors. *Nat Genet*, 45, 104-108.
- Brown, S. M. & Moore, M. 2012. The International Mouse Phenotyping Consortium: past and future perspectives on mouse phenotyping. *Mammalian Genome*, 23, 632-640.
- Carette, J. E., Guimaraes, C. P., Wuethrich, I., Blomen, V. A., Varadarajan, M., Sun, C., Bell, G., Yuan, B., Muellner, M. K., Nijman, S. M., Ploegh, H. L. & Brummelkamp, T. R. 2011. Global gene disruption in human cells to assign genes to phenotypes by deep sequencing. *Nat Biotech*, 29, 542-546.
- Finley, L. W. S., Lee, J., Souza, A., Desquiret-Dumas, V., Bullock, K., Rowe, G. C., Procaccio, V., Clish, C. B., Arany, Z. & Haigis, M. C. 2012. Skeletal muscle transcriptional coactivator PGC-1 α mediates mitochondrial, but not metabolic, changes during calorie restriction. *Proceedings of the National Academy of Sciences*, 109, 2931-2936.